

# SEARCH FOR EXOTIC PHYSICS WITH THE CMS DETECTOR AT THE LHC\*

KATARZYNA ROMANOWSKA-RYBIŃSKA

on behalf of the CMS Collaboration

National Centre for Nuclear Research, High Energy Physics Division  
Hoża 69, 00-681 Warszawa, Poland

*(Received May 7, 2013)*

In this paper, we present strategies and results of eight searches for exotic physics performed by the CMS experiment with 2011 and 2012  $pp$  collision data taken at LHC energy  $\sqrt{s}$ , respectively, 7 TeV and 8 TeV. Among them there are searches for heavy gauge bosons  $W'$  and  $Z'$ , heavy neutrinos, heavy quarks, Kaluza–Klein gravitons, long-lived particles, quark and lepton compositeness, microscopic black holes and a number of exotic dijet resonances such as excited quarks.

DOI:10.5506/APhysPolB.44.1569

PACS numbers: 04.60.Bc, 14.80.-j, 14.65.Jk, 14.70.Pw

## 1. Introduction

The search of physics Beyond the Standard Model (BSM) is one of the main goals of the CMS experiment [1] at the Large Hadron Collider. These searches are traditionally divided into two main groups: searches for Supersymmetry (SUSY) and non-SUSY searches. The latter group is usually referred to as exotic searches. It includes not only theories and models very different from SUSY, like extra dimensions, quarks and leptons compositeness, but also special cases of SUSY, like Gauge Mediated SUSY Breaking (GMSB), predicting the existence of long-lived stau in some regions of the parameter space.

## 2. Searches for microscopic black holes

The possibility of microscopic black hole production in proton–proton collisions at the LHC energy  $\sqrt{s} = 8$  TeV is predicted by theories with low-scale quantum gravity, which are motivated mainly by hierarchy problem,

---

\* Presented at the Cracow Epiphany Conference on the Physics After the First Phase of the LHC, Kraków, Poland, January 7–9, 2013.

that is a large difference between the electroweak scale ( $\sim 0.1$  TeV) and the Planck scale ( $M_{\text{Pl}} \sim 10^{16}$  TeV). Among them there are the ADD model, also known as the model with large extra dimensions, and the Randall–Sundrum model with a single warped extra dimension.

In the ADD model, the fields of the Standard Model (SM) are confined to a four-dimensional membrane, while gravity propagates in  $n$  additional spatial dimensions, compacted on an  $n$ -dimensional torus or sphere of radius  $R$ . Planck scale in  $4 + n$  dimensions ( $M_{\text{D}}^{n+2} \sim M_{\text{Pl}}^2 R^{-n}$ ) is much lower than  $M_{\text{Pl}}$  seen by the  $3 + 1$  dimensional observer. The black holes can be created at the LHC because the energy threshold for their creation is defined by the multidimensional Planck scale  $M_{\text{D}}$ , not  $M_{\text{Pl}}$ .

Once produced, the microscopic black holes decay thermally via Hawking radiation, with equal probabilities to all SM degrees of freedom, that is mainly to quarks and gluons ( $\sim 75\%$ ), due to their color charge. The remaining fraction consists of leptons,  $W$  and  $Z$  bosons, photons and possibly Higgs bosons. Consequently, the signature of a decaying microscopic black hole is the presence of multiple high energy jets, leptons and photons. The CMS searched for excess of such events using  $3.7 \text{ fb}^{-1}$  of 2012 data [2].

In the search for microscopic black holes the best variable to distinguish between the signal and background, which at the same time stays model-independent, is  $S_{\text{T}}$ , the transverse energy of the event.  $S_{\text{T}}$  is defined as a scalar sum of the transverse momenta  $p_{\text{T}}$  of all the jets, leptons and photons with  $p_{\text{T}} > 50$  GeV not overlapping with each other, and the missing transverse energy  $E_{\text{T}}^{\text{miss}}$ . All these objects, except  $E_{\text{T}}^{\text{miss}}$ , are counted towards the final state multiplicity  $N$ .

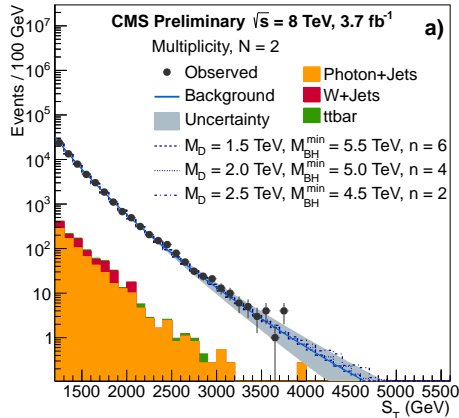


Fig. 1. Distribution of the total transverse energy  $S_{\text{T}}$  for the events with multiplicity  $N = 2$ . The solid line is the background prediction derived from the data in the fit region of 1200–2800 GeV.

The main source of background in this search, which is the most significant at large  $S_T$ , is QCD multijet production. It is estimated from data using the  $S_T$  multiplicity invariance method. This method relies on the independence of the shape of the  $S_T$  spectrum on  $N$ , which is obtained from low  $N$  samples (Fig. 1), and then used for high  $N$  samples (Fig. 2). Smaller backgrounds come from vector-boson + jets and  $t\bar{t}$ , and are negligible at large values of  $S_T$ . Their contribution is estimated from MC simulation.

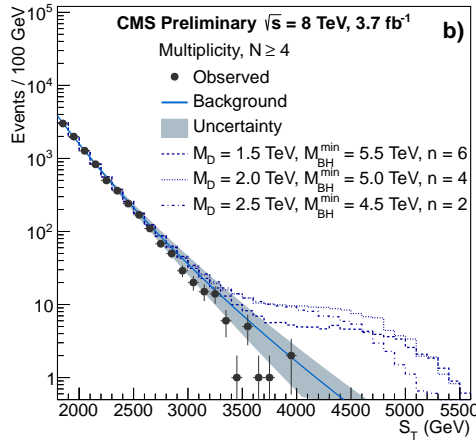


Fig. 2. Distribution of the  $S_T$  for the events with  $N \geq 4$ . The shape of the  $S_T$  distribution is taken from  $N = 2$  sample, normalized to the observed data in the range 1800–2200 GeV.

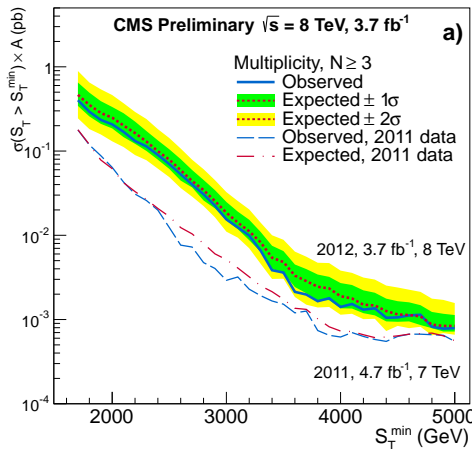


Fig. 3. Model-independent upper cross-section limits for counting experiment with  $S_T > S_T^{\min}$  for events with  $N \geq 3$ .

Since no excess is observed above predicted background, the limits on the black hole production are set. Model independent limits on the cross section times the branching ratio into a multiparticle final state are presented in Fig. 3. Further, the results are interpreted in terms of a set of benchmark semiclassical black hole models (Fig. 4).

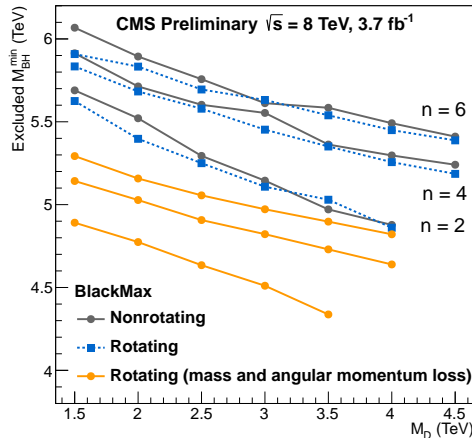


Fig. 4. Minimum excluded black hole mass as a function of  $M_D$  for models without the stable remnant.

### 3. $W'$ leptonic decays

The excess of events with a charged lepton and a neutrino could be the sign of the existence of a new heavy boson, which is postulated by various extensions of the SM, such as Sequential Standard Model (SSM) and split Universal Extra Dimensions (split-UED). In split-UED model, SM particles have corresponding Kaluza–Klein (KK) partners, namely  $W_{KK}^n$ , where  $n$  denotes the  $n$ th KK excitation mode. Due to the KK-parity conservation, only KK-even modes of  $W_{KK}^n$  couple to SM fermions, moreover, only the mode  $n = 2$  offers cross sections large enough for the model to be accessible at the LHC energy  $\sqrt{s} = 8$  TeV.

Another exotic scenario with this signature is quark and lepton compositeness. At energies much lower than  $\Lambda$ , which is the binding energy scale of the fundamental constituents called preons, the compositeness would manifest itself as a four-fermion contact interaction (CI). The signature investigated here requires contact interactions between two quarks, a neutrino and a charged lepton, as described by the helicity-non-conserving (HNC) model.

The CMS searched for  $W'$  bosons and compositeness using combined 7 TeV and 8 TeV datasets with integrated luminosities of  $5.0 \text{ fb}^{-1}$  and  $3.7 \text{ fb}^{-1}$  respectively [3]. In this analysis, the main discriminating variable is the transverse mass  $M_T$  of the lepton- $E_T^{\text{miss}}$  system, calculated as

$$M_T = \sqrt{2 p_T^l E_T^{\text{miss}} (1 - \cos \Delta\phi_{l,\nu})}, \quad (1)$$

where  $\phi_{l,\nu}$  is the azimuthal angle between the charged leptons transverse momentum  $p_T^l$  and the  $E_T^{\text{miss}}$  direction. In all the models considered, the lepton and  $E_T^{\text{miss}}$  are expected to be almost back-to-back in the transverse plane, and balanced in transverse energy, what allows to introduce additional kinematic criteria in the event selection:  $0.4 < p_T^l/E_T^{\text{miss}} < 1.5$  and  $|\phi_{l,\nu} - \pi| < 0.2\pi$ .

The main source of SM background is off-peak, high- $M_T$  tail of the SM  $W \rightarrow l\nu$  decays. Smaller contributions arise from  $t\bar{t}$ , the Drell–Yan (DY), and diboson events. Another important background comes from QCD multijet processes, but it is largely removed by the analysis selections. Contributions from events with  $\tau$  decaying to leptons were considered as well, but were found to be negligible. Figure 5 shows observed lepton- $E_T^{\text{miss}}$  transverse mass distributions in the electron and muon channels.

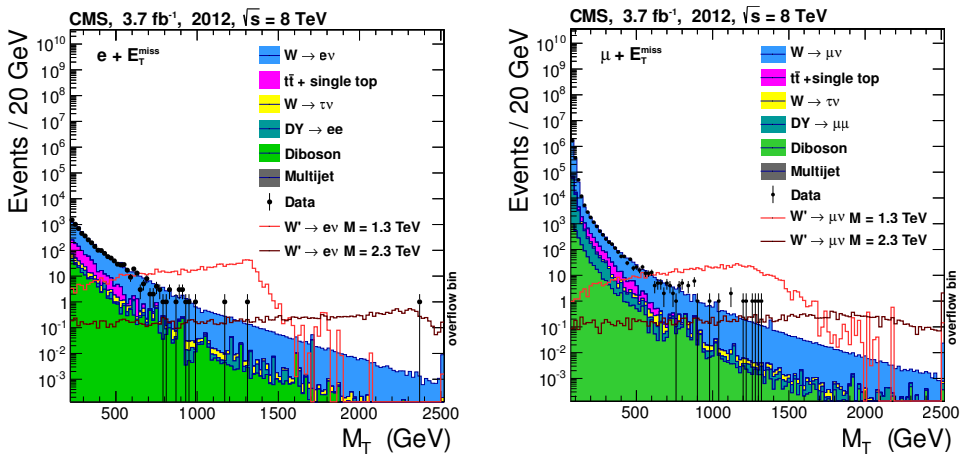


Fig. 5. Observed lepton- $E_T^{\text{miss}}$  transverse mass distributions in the electron (left) and the muon (right) channel. Simulated signal distributions for a SSM  $W'$  are also shown, including detector resolution effects.

No evidence was found for the excess of events with a charged lepton and a neutrino. The limits on a heavy charged gauge boson are presented in Fig. 6. The four-fermion contact interaction of the HNC model is excluded for values of  $\Lambda < 10.5$  TeV in the electron channel and  $\Lambda < 8.8$  TeV in the muon channel. The bounds on the split-UED parameter space,  $(1/R, \mu)$  are shown in Fig. 7.

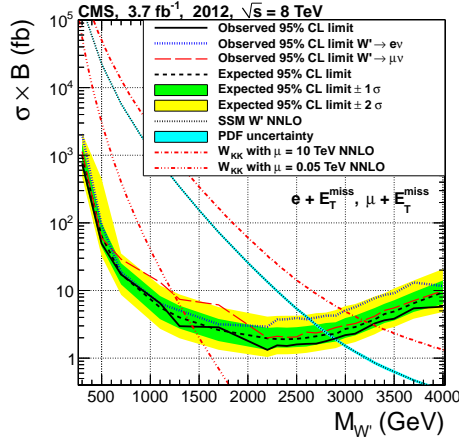


Fig. 6. Limits on the cross section times the single channel branching fraction  $\sigma \times B$  for heavy  $W'$  bosons for the electron and the muon channels.

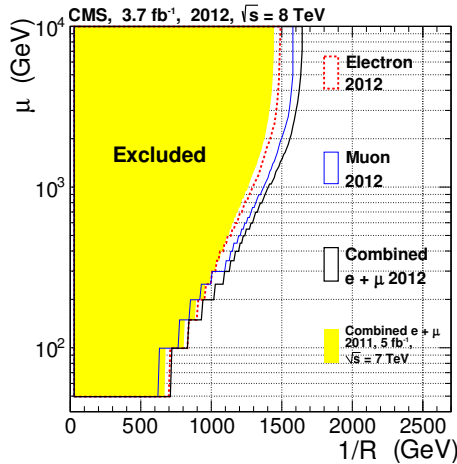


Fig. 7. The limits on the split-UED parameters  $\mu$  and  $1/R$  derived from the  $W'$  mass limits taking into account the corresponding width of the  $W'_{KK}{}^{n=2}$ .

#### 4. Dilepton resonances

Many theories of BSM physics predict the existence of heavy narrow resonances that decay to lepton pairs. Among them there are already mentioned SSM, superstring inspired Grand Unified Theories (GUT), and the Randall–Sundrum (RS) model of extra dimensions. In the first two models, the heavy resonance is  $Z'$ , denoted respectively  $Z'_{\text{SSM}}$  and  $Z'_{\psi}$ , while in the third it is the Kaluza–Klein graviton.

The CMS searched for such objects using combined 7 TeV and 8 TeV datasets with integrated luminosities of up to  $5.3 \text{ fb}^{-1}$  and  $4.1 \text{ fb}^{-1}$  respectively [4].

The main source of background in this search is DY production. It is estimated using both MC simulation and data. The shape of distribution is taken from MC, and it is normalized to the isolated same flavor dilepton event count at the  $Z$  peak in data. Smaller background contributions come from other SM processes that produce isolated dileptons. Considered processes are  $t\bar{t}$ ,  $tW$ ,  $Z \rightarrow \tau\bar{\tau}$ , and diboson production. The absolute normalization and shape for these backgrounds are taken directly from MC. Another source of background are jets misreconstructed as leptons (significant in dielectron channel) and cosmic muons. Both contributions are estimated from data. The dilepton mass distributions with the SM background prediction are shown in Fig. 8.

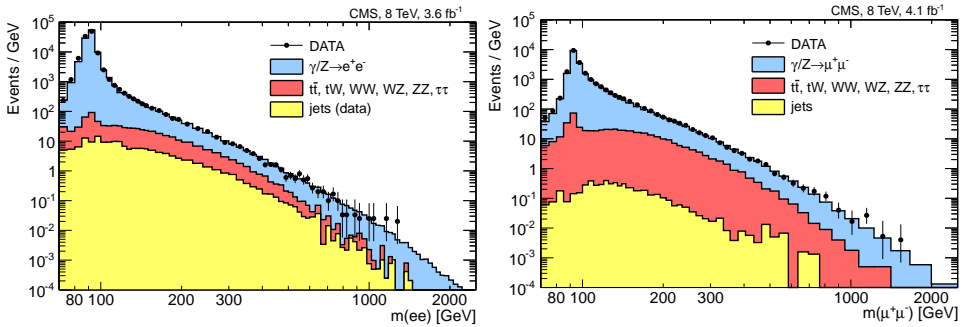


Fig. 8. The invariant mass spectrum of  $\mu^+\mu^-$  (left) and  $e^+e^-$  (right) events for the  $\sqrt{s} = 8 \text{ TeV}$  data set. The points with error bars represent the data. The solid histograms represent the standard model predicted background contributions.

These distributions were used to perform a shape-based analysis, robust against uncertainties in the absolute background level. The data proved to be consistent with expectations from the SM. The limits are set on the ratio ( $R_\sigma$ ) of the production cross sections times branching fractions of a heavy narrow resonance to that of the  $Z$  boson, which eliminated many experimental and theoretical uncertainties cancelling in this ratio. These limits are further translated into lower limits on the masses of new heavy narrow resonances, which are presented in Fig. 9. The results are applicable to any model with a narrow resonance that has equal dimuon and dielectron branching fractions.

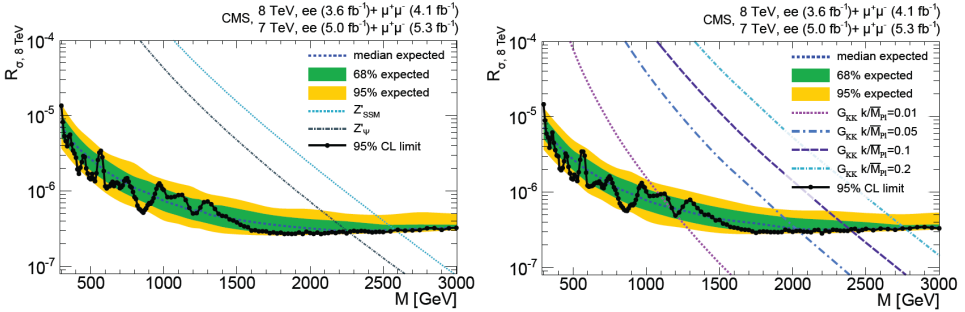


Fig. 9. Upper limits on the ratio  $R_\sigma$  of the production cross section times branching fraction into lepton pairs to the same quantity for  $Z$  bosons, as a function of resonance mass  $M$  for spin-1 (left) and spin-2 (right) boson production.

## 5. Dijet resonances

Another group of objects whose existence is predicted by many extensions of the SM are massive particles that couple to quarks or antiquarks and gluons, resulting in resonances in the dijet mass spectrum. The CMS searched for such objects using  $4.0 \text{ fb}^{-1}$  of 2012 data [5].

The following specific models of narrow dijet resonances produced via the  $s$ -channel are considered in this search: string resonances,  $E_6$  diquarks, excited quarks, axigluons, color-octet colorons, the S8 resonance predicted in technicolor models, new gauge bosons ( $W'$  and  $Z'$ ) and RS gravitons.

This analysis is very sensitive to gluon radiation. In order to reduce this sensitivity, a special jet reconstruction technique is used, which combines Particle Flow into “wide jets”. The algorithm works in the following way: first two jets of the highest  $p_T$  are selected, then the Lorentz vectors of all other jets are added to the closest of these two jets, if within  $\Delta R = \sqrt{\Delta\eta^2 + \Delta\phi^2} < 1.1$ . The particles belonging to the jets can extend further up to 1.6. The four-momentum of each wide jet is computed as the sum of the four-momenta of the constituent jets. To suppress background events coming from QCD processes, two wide jets must be separated by  $|\Delta\eta_{jj}| < 1.3$ , each jet inside the region  $|\eta| < 2.5$ . The dijet mass is calculated as

$$m_{jj} = \sqrt{(E_{j1} + E_{j2})^2 - |\vec{p}_{j1} + \vec{p}_{j2}|^2}, \quad (2)$$

where  $E_{ji}$  and  $\vec{p}_{ji}$  ( $i = 1, 2$ ) are the energy and the momentum of a wide jet. Only events with  $m_{jj} > 890 \text{ GeV}$  are selected. The dijet mass spectrum from wide jets is presented in Fig. 10. It is fitted with a smooth, empirical parameterization which well describes the prediction from simulated QCD dijet events.



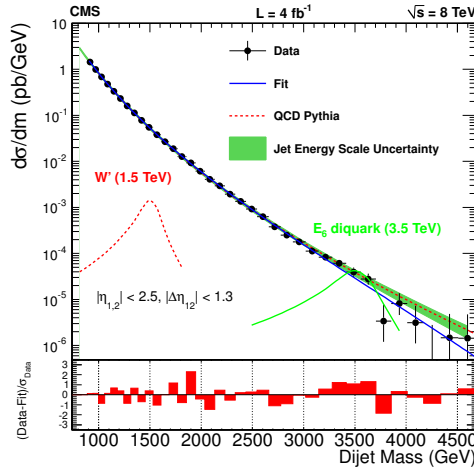


Fig. 10. The dijet mass spectrum from wide jets (points) compared with a smooth fitted curve (solid line) and with the predicted QCD background (dashed line).

No significant evidence for narrow resonance production is observed. Upper limits are set on the production cross section of hypothetical new particles decaying to quark–quark, quark–gluon, or gluon–gluon final states. These limits are then translated into lower limits on the masses of new resonances in specific scenarios of the BSM physics. The results can be applied to all new particles for which the natural resonance width is small compared to the CMS dijet mass resolution.

TABLE I

Observed and expected exclusions at the 95% C.L. on the mass of various resonances.

Model	Final state	Observed excluded mass range [TeV]	Expected excluded mass range [TeV]
String resonance	$qg$	[1.0, 4.78]	[1.0, 4.75]
Excited quark	$qg$	[1.0, 3.19]	[1.0, 3.47]
$E_6$ diquark	$qq$	[1.0, 4.28]	[1.0, 4.16]
Axigluon/coloron	$q\bar{q}$	[1.0, 3.27]	[1.0, 3.60]
S8 resonance	$gg$	[1.0, 2.79]	[1.0, 2.54]
$W'$ boson	$q\bar{q}$	[1.0, 1.73]	[1.0, 1.97]
$Z'$ boson	$q\bar{q}$	[1.0, 1.62]	[1.0, 1.58]
RS graviton	$q\bar{q} + gg$	[1.0, 1.45]	[1.0, 1.29]

## 6. Heavy neutrino

After recent observation of neutrino oscillation, the SM assumption that neutrinos are massless no longer holds. Left–Right Symmetric Extensions (LRSM) to the SM ( $SU_C(3) \otimes SU_L(2) \otimes SU_R(2) \otimes U(1)$ ) solve this problem introducing neutrino masses, but they also imply the existence of massive right-handed neutrinos  $N_l$  ( $l = e, \mu, \tau$ ) and three additional gauge bosons  $W_R^\pm$  and  $Z'$ . These extensions were originally proposed to explain the origin of parity non-conservation in weak interactions.

The leading production mode of the heavy neutrinos at the LHC is the reaction  $pp \rightarrow W_R + X \rightarrow N_l + l + X$ , where  $l = e, \mu$ .  $N_l$  decays into a charged lepton and an off-shell  $W_R$  which subsequently decays into a pair of quarks which hadronize into jets

$$W_R \rightarrow l_1 N_l \rightarrow l_1 l_2 W_R^* \rightarrow l_1 l_2 q q' \rightarrow l_1 l_2 j j. \quad (3)$$

A unique feature of the  $N_l$  production and decay process is that it has a two-dimensional resonance structure. The distributions of the variables  $M_{lljj}$  and  $M_{l_2jj}$  should exhibit narrow peaks.  $W_R$  and  $N_l$  masses vary independently.

The CMS searched for heavy right-handed neutrinos using  $3.6 \text{ fb}^{-1}$  of  $pp$  collision data collected in 2012 at  $\sqrt{s} = 8 \text{ TeV}$  [6]. In the analysis, the  $W_R$  candidates are assembled from two high  $p_T$  jets and two high  $p_T$ , electrons or muons, isolated from jets in a cone  $\Delta R(l, j) < 0.5$ . To limit the impact of SM background processes, only the events with a minimum dilepton mass  $M_{ll} = 200 \text{ GeV}$  are selected. The signal region starts at the four-object mass  $M_{lljj} = 600 \text{ GeV}$ .

The main source of background are SM processes with two real leptons, such as  $t\bar{t}$  and  $Z$ +jets, estimated using reconstructed  $e\mu jj$  events in data, but there is also a small contribution from QCD multijet events due to jets misidentified as isolated leptons, which is also estimated from data. The  $Z$ +jets background contribution is estimated from MC simulation of DY production in association with jets. It is normalized by scaling the simulated  $M_{ll}$  distribution to data in a window  $60 < M_{ll} < 120$ . Additional SM background processes:  $W$ +jets, diboson, and single top are modeled using the MC simulation. The  $M_{lljj}$  distributions for electron and muon channels are presented in Fig. 11.

No excess over expectations from SM processes is observed. The limits are set on  $W_R$  production using the shape analysis of the reconstructed four-object mass distribution. Assuming degenerate neutrino masses for all neutrino flavors, the 8 TeV electron and muon channel results were combined to obtain exclusion in the  $(M_{W_R}, M_{N_l})$  mass plane extending to  $M_{W_R} = 2.8 \text{ TeV}$ . Combining 7 and 8 TeV data for the muon channel only,

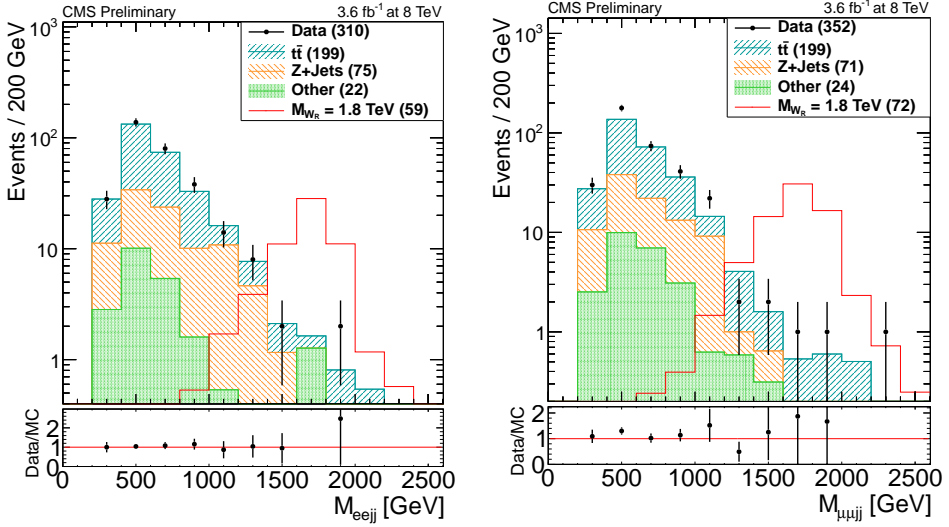


Fig. 11. Four-object mass distribution for  $eejj$  (left) and  $\mu\mu jj$  (right) events surviving event selection criteria, neglecting the  $M_U$  requirement.

and assuming that only  $N_\mu$  is light enough to be produced at the LHC, the  $W_R$  production is excluded up to  $M_{W_R} = 2.9$  TeV. The exclusion limits are presented in Fig. 12.

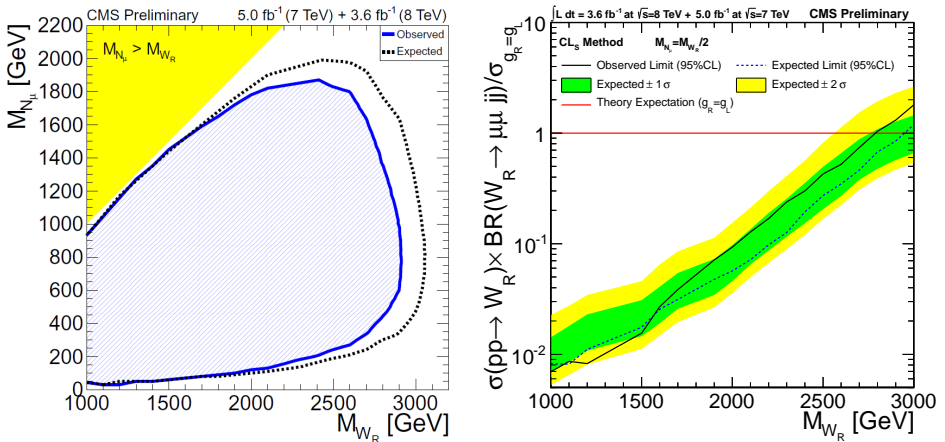


Fig. 12. The 95% confidence level exclusion region in the  $(M_{W_R}, M_{N_l})$  plane (left), and as a function of  $W_R$  mass with  $M_{N_\mu} = \frac{1}{2} M_{W_R}$  (right) obtained combining studies of 7 TeV and 8 TeV  $pp$  collision data.

## 7. Heavy quarks

New heavy quarks  $Q$  that decay to top quarks and electroweak bosons  $W$ ,  $Z$ , or even Higgs bosons appear in many models of the BSM physics. One of them, the simplest, is the sequential fourth generation model.

The CMS searched for the pair production of new heavy quarks  $Q$  that decay exclusively to a top quark and a  $W$  boson, or to a top quark and a  $Z$  boson with  $5.0 \text{ fb}^{-1}$  of 2011 data [7]. The full decay chains for heavy down-type quarks and for up-type quarks are respectively

$$Q\bar{Q} \rightarrow tW^-\bar{t}W^+ \rightarrow bW^+W^-\bar{b}W^-W^+, \quad (4)$$

$$Q\bar{Q} \rightarrow tZ\bar{t}Z \rightarrow bW^+Z\bar{b}W^-Z. \quad (5)$$

In both cases, there are two  $W$  bosons in the final state. In this analysis, one of them is required to decay leptonically and the other hadronically. Only events with exactly one charged lepton, at least four jets and an imbalance in  $p_T$  are selected. At least one jet must be consistent with the decay of the bottom quark.

The background is dominated by  $t\bar{t}$  production, as well as the production of  $W$  bosons with associated jets. These background processes, however, have smaller lepton and jet  $p_T$  and lower jet multiplicities than those in heavy quark decays. Other backgrounds are single top quark, diboson and multijet events.

Selected events are classified based on the number of final-state jets. The main variable, discriminating between signal and background is the scalar sum  $S_T$  of the  $p_T$  of the lepton, the jets, and  $E_T^{\text{miss}}$ .

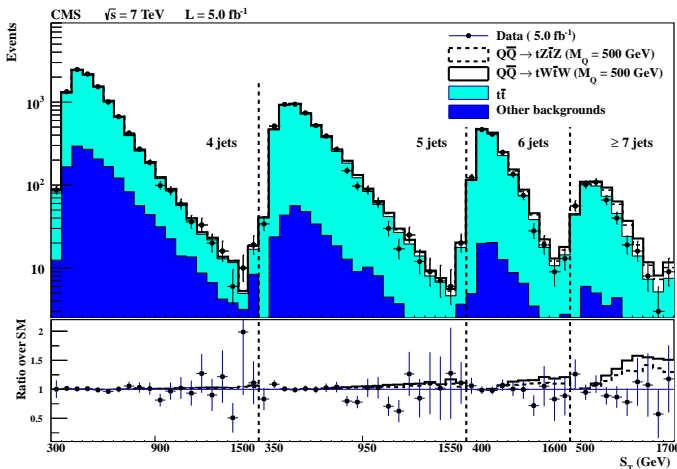


Fig. 13. Distribution in  $S_T$  for different  $N_J$  after the maximum-likelihood fit to data. The bottom plot shows the ratios of data and SM plus signal over SM.

The search for a  $Q\bar{Q}$  signal is performed by fitting the data to the distribution of the  $S_T$  as a function of jet multiplicity  $N_J$ . The fit is done for the combination of  $e$ +jets and  $\mu$ +jets channels and for  $N_J = 4, 5, 6$ , and 7 jets. The distributions in  $S_T$  for different  $N_J$  are presented in Fig. 13.

No significant excess of events is observed with respect to the SM expectations. Assuming a strong pair-production mechanism, quark masses below 675 (625) GeV decaying into  $tW$  ( $tZ$ ) are excluded. The exclusion limits are presented in Fig. 14.

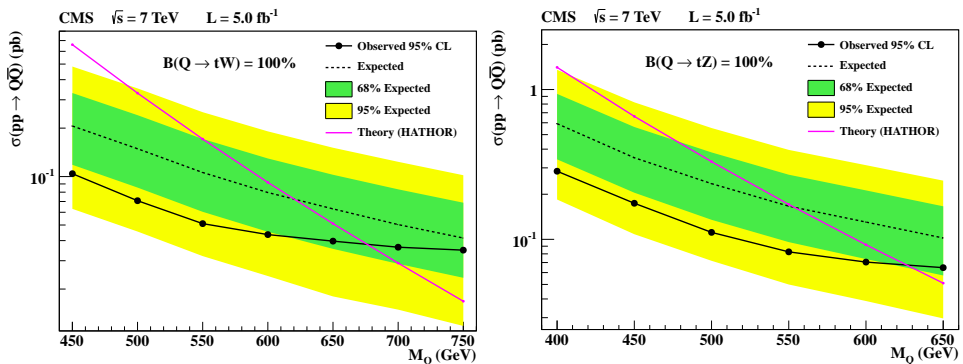


Fig. 14. The observed and the expected 95% C.L. upper limits on the  $Q\bar{Q}$  production cross section as a function of the heavy quark mass,  $M_Q$ , compared to the theoretical  $Q\bar{Q}$  cross section for the case of a down-type heavy quark decaying exclusively to  $tW$  (left), and for the case of an up-type heavy quark decaying exclusively to  $tZ$  (right).

## 8. $Z' \rightarrow t\bar{t}$

Among many still open questions of the SM there is the mechanism of electroweak symmetry breaking. One of the models providing the explanation of this problem is topcolor-assisted technicolor (TC2). It explains not only the electroweak symmetry breaking but also flavor symmetry breaking, giving masses to the weak gauge bosons and fermions. One of the scenarios of TC2 predicts the existence of a heavy boson  $Z'$  with preferential couplings to the third quark generation and with no significant couplings to the leptons (leptophobic).

The CMS searched for topcolor leptophobic  $Z' \rightarrow t\bar{t}$  resonance with  $5 \text{ fb}^{-1}$  of 2011  $pp$  collisions data in the  $2l + 2\nu$ +jets final state, where  $l = e, \mu$  [8]. In this  $t\bar{t}$  decay topology, each top quark decays to a  $W$  boson and a  $b$  quark, and subsequently, each  $W$  boson decays into a lepton and a neutrino, so selected events contain two oppositely charged, isolated leptons

with high  $p_T$ , large momentum imbalance due to two undetected neutrinos, and at least two jets. Events were separated into three channels based on lepton flavor:  $ee$ ,  $\mu\mu$ , and  $e\mu$ .

The main sources of background in this search are  $t\bar{t}$ , DY, single top and diboson events. There are also minor contributions from  $W \rightarrow l\nu$  and multijet production. The background coming from SM  $t\bar{t}$ , DY, and  $W \rightarrow l\nu$  was estimated using MC simulation. DY background contribution was obtained from MC simulation and normalized to the data DY-enriched sample in the region of  $76 < M_{ll} < 106$  GeV. The source of the multijet background are misidentified leptons or genuine leptons from semi-leptonic decays of  $b/\bar{b}$  or  $c/\bar{c}$  quarks, which pass the isolation requirement. This contribution is determined from data by inverting the isolation criteria for both leptons, and then extrapolating that yield to the signal region.

The  $t\bar{t}$  invariant mass is constructed using the four-vectors of the two leading leptons, the two leading jets, and the  $E_T^{\text{miss}}$ . Additionally, to provide a more powerful discriminant between backgrounds and the  $Z'$  signal than that based on invariant mass alone a multivariate analysis, based on Bayesian neural networks (BNN) has been carried out. The distributions of the  $t\bar{t}$  invariant mass and the BNN output discriminant are presented in Fig. 15.

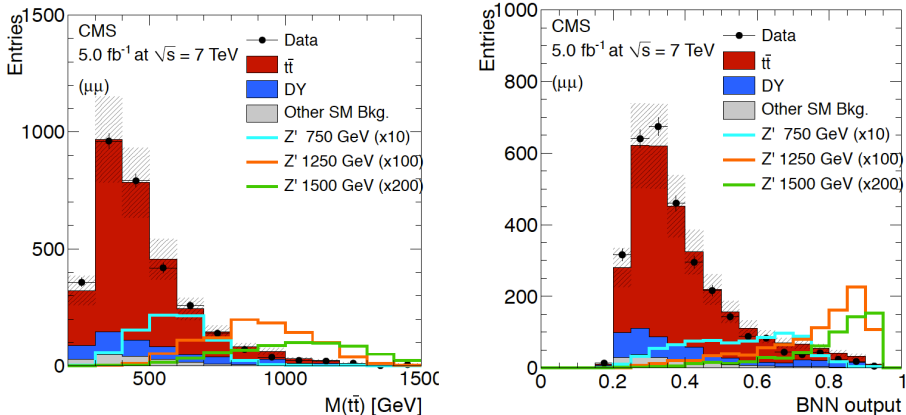


Fig. 15. Distributions the  $t\bar{t}$  invariant mass (left) and of the BNN output discriminant (right) for the  $\mu\mu$  channel. The  $Z'$  signal corresponds to a resonance width of  $\Gamma_{Z'} = 0.012 M_{Z'}$ , and has been scaled up so as to be visible.

No significant deviations from the SM background are observed. The upper limits on  $\sigma_{Z'}\mathcal{B}(Z' \rightarrow t\bar{t})$  for different values of  $M_{Z'}$  are set using the CLs criteria. Using the BNN distribution improves the expected limit by 29% compared to the invariant mass distribution, that is why the more sensitive BNN technique is used. The resulting expected limits and the observed limits are shown in Fig. 16.

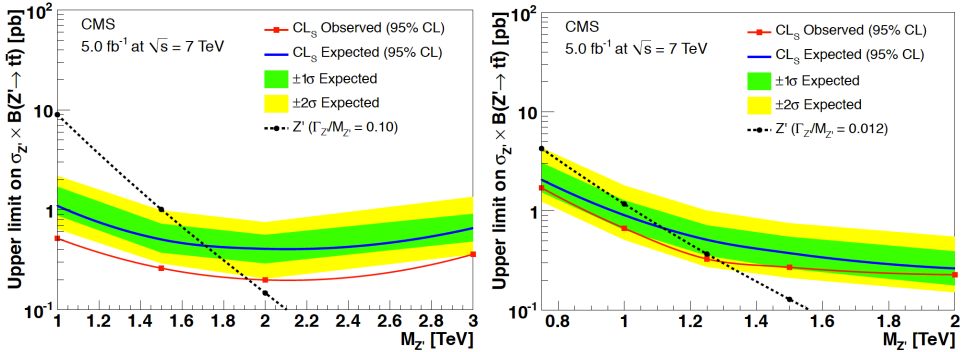


Fig. 16. Upper limits on  $\sigma_{Z'}B(Z' \rightarrow t\bar{t})$  versus  $M_{Z'}$  for narrow and wide resonances. Also shown is the theoretical prediction for the  $Z'$ .

## 9. Heavy long-lived charged particles

Most of the exotic searches are directed at particles promptly decaying to SM particles. This search, on the other hand, aims at direct detection of exotic objects — heavy long-lived charged particles, here referred to as Heavy Stable Charged Particles (HSCP). Such particles can be detected at the CMS as high momentum ( $p$ ) tracks with an anomalously large energy loss through ionization ( $dE/dx$ ) and an anomalously long time-of-flight (TOF). Various extensions to the SM predict the existence of such particles, which are long-lived as a result of a new conserved quantum number, a kinematic constraint or a weak coupling.

Among these models is SUSY, where HSCP can be scalar tau — stau  $\tilde{\tau}$  (minimal Gauge-Mediated SUSY breaking model — GMSB) as well as gluino  $\tilde{g}$  or scalar top quark  $\tilde{t}$  hadronizing to  $\tilde{g}$ -gluon state ( $R$ -gluonball) or  $R$ -hadron. There is also a new model that postulates a QCD-like confinement force between new elementary particles (hyper-quarks) and which are the constituents of long-lived hyper-mesons, such as hyper- $\pi$  ( $\tilde{\pi}$ ), hyper- $K$  ( $\tilde{K}$ ), or hyper- $\rho$  ( $\tilde{\rho}$ ).  $\tilde{\pi}$  and  $\tilde{K}$  are produced in pairs either via the DY process or via production of a resonant  $\tilde{\rho}$  ( $\tilde{\rho} \rightarrow \tilde{K}\tilde{K}$ ). This search [9] is based on two measurements that were developed specially for this purpose: the  $dE/dx$  measurement provided by the silicon strip and pixel detectors, and the TOF measured by muon chambers.

The estimate of the compatibility of the observed particle charge loss measurements with those expected for particles close to the minimum of ionization is the  $I_{\text{as}}$ , which is a modified version of the Smirnov–Cramer–von Mises discriminant

$$I_{\text{as}} = \frac{3}{J} \times \left\{ \frac{1}{12J} + \sum_{i=1}^J \left[ P_i \times \left( P_i - \frac{2i-1}{2J} \right)^2 \right] \right\}, \quad (6)$$

where  $J$  is the number of track measurements in the silicon strip detectors,  $P_i$  is the probability for a particle close to the minimum of ionization to produce a charge smaller or equal to that of the  $i$ th measurement for the observed path length in the detector, and the sum is over the track measurements ordered in terms of increasing  $P_i$ .

The TOF measurement of the candidate track is calculated from the differences ( $\delta_t$ ) between the particle chamber crossing time and the average time at which a high momentum muon, produced at the collision point would pass through the same chamber. The HSCPs would have  $\delta_t$  greater than zero. The  $\beta^{-1}$  for a single measurement is calculated via the equation

$$\beta^{-1} = 1 + \frac{c\delta_t}{L}, \quad (7)$$

where  $L$  is the flight distance and  $c$  is the speed of light. The track  $\beta^{-1}$  value is calculated as the weighted average of the  $\beta^{-1}$  measurements associated with the track.

The analysis uses two offline selections referred to as tracker-only and tracker + TOF. The first is applicable to the particles that are likely to flip or lose charge, and thus may not reach the muon chambers, and the second to the muon-like particles. The search is performed as a counting experiment in a mass window that depended on the HSCP mass hypothesis,  $M$ , and the model of interest.

To estimate the SM background the ABCD method is used. This method exploits the non-correlation between the  $p_T$ ,  $dE/dx$  and TOF measurements. A loose selection is defined such that there is a relatively large number of background candidates in the signal region. This selection allows a cross-check on the accuracy of the background prediction to be performed (Fig. 17).

After comparing data in the signal region with the expected background no statistically significant excess was observed. The observed data sample was used to calculate upper limits on the HSCP production cross section for each considered model and mass point. The cross section upper limit curves obtained the tracker + TOF selection are shown in Fig. 18, along with the theoretical predictions for the chosen signal models.



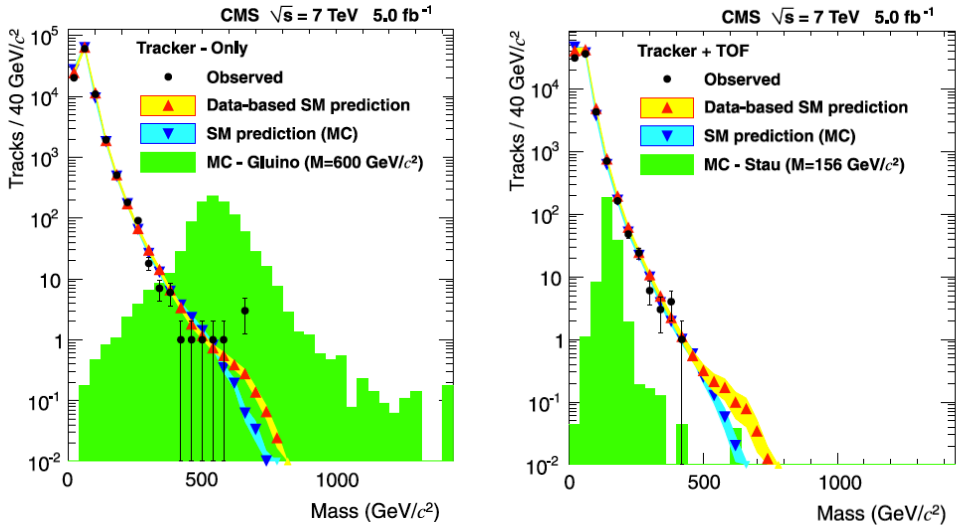


Fig. 17. Distribution of the candidate mass for the loose selection, for the tracker only (left) and tracker + TOF (right) candidates.

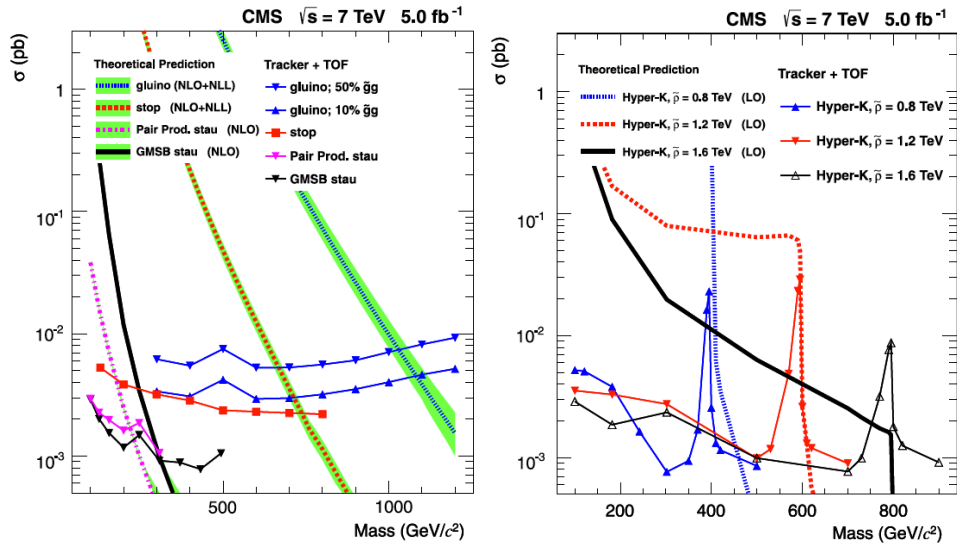


Fig. 18. Predicted theoretical cross section and observed 95% C.L. upper limits on the cross section for the different signal models considered: production of  $\tilde{t}$ ,  $\tilde{g}$  and  $\tilde{\tau}$  (left) and the  $\tilde{K}$  models with different  $\tilde{\rho}$  mass values (right).

## 10. Conclusions

The CMS experiment has an extensive, constantly growing program to search for the BSM physics. The data collected in 2011 and 2012 allowed to exclude wide ranges of masses and production cross sections of many different exotic particles.

This work was partially supported by the National Science Centre (Poland) grant N N202 167440.

## REFERENCES

- [1] CMS Collaboration, *JINST* **3**, S08004 (2008).
- [2] CMS Collaboration, “Search for Microscopic Black Holes at  $\sqrt{s} = 8$  TeV with the CMS Detector”, CMS PAS EXO-10-009.
- [3] CMS Collaboration, *Phys. Rev.* **D87**, 072005 (2013) [arXiv:1302.2812 [hep-ex]].
- [4] CMS Collaboration, *Phys. Lett.* **B720**, 63 (2013) [arXiv:1212.6175 [hep-ex]].
- [5] CMS Collaboration, arXiv:1302.4794 [hep-ex].
- [6] CMS Collaboration, “Search for a Heavy Neutrino and Right-handed  $W$  of the Left–Right Symmetric Model in  $pp$  Collisions at  $\sqrt{s} = 8$  TeV”, CMS PAS EXO-12-017.
- [7] CMS Collaboration, *J. High Energy Phys.* **01**, 154 (2013) [arXiv:1210.7471 [hep-ex]].
- [8] CMS Collaboration, *Phys. Rev.* **D87**, 072002 (2013) [arXiv:1211.3338 [hep-ex]].
- [9] CMS Collaboration, *Phys. Lett.* **B713**, 408 (2012).